Journal of Alloys and Compounds 503 (2010) 10–18

Contents lists available at ScienceDirect

Journal of Alloys and Compounds

journal homepage: www.elsevier.com/locate/jallcom

Electronic and optical properties of alkali metal selenides in anti-CaF_2 crystal structure from first-principles

S.M. Alay-e-Abbas[a], N. Sabir[a], Y. Saeed[b], A. Shaukat[c,*]

[a] Department of Physics, GC University, Allama Iqbal Road, Faisalabad 38000, Pakistan
[b] Institute of Physical Biology, South Bohemia University, Nove Hrady 37333, Czech Republic
[c] Department of Physics, University of Sargodha, Sargodha, Pakistan

ARTICLE INFO

Article history:
Received 8 February 2010
Received in revised form 1 May 2010
Accepted 3 May 2010
Available online 11 May 2010

Keywords:
Alkali metal selenides
First-principles calculations
FP-LAPW
Electronic and optical properties
Generalized gradient approximation

ABSTRACT

We have performed FP-LAPW calculations in the framework of density functional theory (DFT) to compute ground-state electronic and optical properties of alkali metal selenides M_2Se [M: Li, Na, K, Rb] in anti-CaF_2 crystal structure. The generalized gradient approximation (GGA) parameterization schemes proposed by Wu and Cohen (WC) and Engel and Vosko (EV) have been utilized for these calculations and some trends in the electronic properties of alkali metal selenides have been analyzed in the light of available theoretical and experimental data of other group IA–VI crystals. Electronic density of states for these compounds has been obtained to elucidate contribution from different anion and cation states to the electronic structure. Optical properties such as complex dielectric function $\varepsilon(\omega)$, absorption coefficient $I(\omega)$, refractive index $n(\omega)$, extinction coefficient $k(\omega)$ and reflectivity $R(\omega)$ for incident photon energy up to 35 eV and energy-loss functions have been predicted for M_2Se compounds. Various interband transitions and the possible contributions of the cation and anion states to these transitions have been presented.

1. Introduction

The oxides (M_2O) and chalcogenides (M_2Ch) of alkali metals [M: Li, Na, K, Rb; Ch: S, Se, Te] constitute a crystalline family that has shown great technological usefulness in devices requiring high ionic conductivity and large fundamental energy band gaps. Apart from being used in power sources, fuel cells, gas-detectors and ultra violet space technology devices, these ionic compounds also play important role in the development of photocathode, in supporting catalytic reactions and enhancing oxidation of semiconductor surfaces [1–8]. At room temperature these compounds crystallize into a stable anti-CaF_2 (anti-fluorite) structure type [9–10] (space group $Fm\bar{3}m$). The CaF_2 (calcium fluoride) compound has a basic crystalline structure that consists of a face-centered cubic packing of Ca cations, with F anions located in all the Ca tetrahedral. Whereas, the anti-morphous to the CaF_2 structure has exchanged positions of the cations and anions, and is known as the anti-fluorite type structure. In the M_2Se [M: Li, Na, K, Rb] compounds, the metal atoms (M) are located at (0.25; 0.25; 0.25) and (0.75; 0.75; 0.75) and the selenium atoms (Se) are located at (0; 0; 0) as shown in Fig. 1.

Unlike the oxide and sulfide compounds of this crystal family, the selenides of alkali metals have received less investigative attention from researchers towards their electronic and optical traits. Most of the research work for alkali metal selenides has been confined to studying the structural properties of these materials [11–14]. However, no theoretical and experimental account of the electronic and optical properties of these materials was available in literature until recently when Eithiraj et al. [15] utilized the Tight-Binding Linear Muffin-Tin Orbitals (TB-LMTO) method to investigate ground-state and under compression electronic behavior of selenides and tellurides of Li, Na and K.

In order to understand and enhance our knowledge of the electronic and optical properties of these materials and motivated by their inalienable importance among binary crystals, we have carried out self-consistent density functional calculations within the generalized gradient approximation (GGA) using the Full Potential Linearized Augmented Plane Wave (FP-LAPW) method. Calculated ground-state structural properties of the aforementioned crystals have been compared with available theoretical and experimental data. Moreover, features of the electronic band structures and optical parameters of alkali metal selenides have been analyzed in the light of available theoretical and experimental data of other group IA–VI crystals. The results for M_2Se compounds presented in this paper may provide reference for future experimental as well as theoretical studies related to these ionic materials and their intricate compounds.

* Corresponding author. Tel.: +92 48 9230618; fax: +92 48 9230671.
E-mail address: schaukat@gmail.com (A. Shaukat).

0925-8388/$ – see front matter © 2010 Elsevier B.V. All rights reserved.
doi:10.1016/j.jallcom.2010.05.014

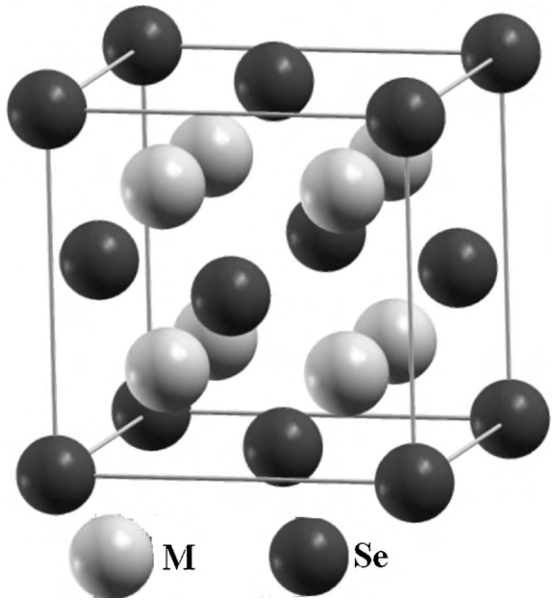

Fig. 1. Atomic structure of the anti-CaF_2-type M_2Se showing the face-centered cubic packing of (Se) anions, with (M) anions located in all the Se tetrahedral.

2. Calculational details and structural optimization

The density functional calculations for M_2Se ionic crystals were performed using the FP-LAPW method in the framework of density functional theory (DFT) as implemented in the WIEN2K code [16]. In these calculations, an approximate functional is required to determine the exchange-correlation energy (E_{xc}) whose accurate determination ensures the quality of obtained results. A crude determination of E_{xc} can be made with the local density approximation (LDA) [17] that can be readily calculated for a system consisting of homogeneous electron gas. However, in real crystalline solids such is not the case and the valence electron density being inhomogeneous in space, a refined determination of E_{xc} can be achieved by using GGA exchange-correlation functionals. To this end the GGA expression proposed by Wu and Cohen [18] (WC) that performs fourth-order gradient expansion of exchange energy functional has proven most suitable for studying structural properties of solids as compared to the earlier GGA schemes such as the one devised by Perdew–Burke–Ernzerhof [19] (PBE). On the other hand, due to its simple form the WC functional is not flexible enough to accurately determine total exchange-correlation energy and its charge derivative. For this reason the modified GGA form of Engel and Vosko [20] (EV) GGA functional (that produces more accurate exchange-correlation potential at the expense of less accurate exchange energy) can be utilized; that has resulted in providing improved electronic band structure calculations for alkali metal oxides [21] and sulfides [22].

In the FP-LAPW method a muffin-tin model for crystal potential is assumed and the electrons are paired into two groups. The bound electrons have been treated as core electrons whose charge densities are confined within the muffin-tin spheres and the remaining are treated as valence electrons that reside outside the surface of muffin-tin spheres. The wave function, charge density and potential are expanded inside the non-overlapping spheres of muffin-tin radius (R_{MT}) around each species where linear combination of radial solution of the Kohn-Sham equation times the spherical harmonic has been utilized. Plane wave basis set has been utilized in the remaining interstitial space of the unit cell. The muffin-tin sphere radius, R_{MT}, for each species of the compounds under study is so chosen, that there is no charge leakage from the core and total energy convergence is ensured. The R_{MT} values for Li, Na, K, Rb and Se were selected to be 1.6, 2.1, 2.7, 2.9 and 2.8 a.u., respectively. These values have been selected after performing several tests using different muffin-tin radii as well as different sets of **k**-points to ensure convergence of energy. The maximum value of angular momentum ($\mathbf{l}_{max}$) for the wave function expansion inside the atomic spheres has been taken at 10. In the interstitial region the plane wave cut-off value of $\boldsymbol{K}_{max} \times R_{MT} = 9$ has been used for these calculations. A mesh of 72 **k**-points was taken for the Brillion zone integrations in the corresponding irreducible wedge.

Table 1
Lattice parameters a_o (Å), total energy E_0 (Ry), bulk moduli B_o (GPa) and its pressure derivative B' for alkali metal selenide. Results obtained in present work using WC GGA along with available experimental and theoretical values.

		Present work		TB-LMTO[g]	Other theoretical works
		WC GGA	Experimental		
Li_2Se	a_o	5.966	6.017[a,b]	6.030	–
	E_0	−4889.6890	–	−4885.1168	–
	B_o	34.7219	–	34.00	65[d], 35.1[e], 38.1[f]
	B'	3.8557	–	–	–
Na_2Se	a_o	6.796	6.823[a], 6.809[b]	6.755	–
	E_0	−5508.7397	–	−5502.8612	–
	B_o	24.8830	–	27.27	39[d], 22.6[e], 30.7[f]
	B'	4.1790	–	–	–
K_2Se	a_o	7.751	7.92[a], 7.676[b]	7.676	–
	E_0	−7266.9673	–	−7258.9557	–
	B_o	16.5313	–	18.64	24[d], 18.6[e], 21.6[f]
	B'	5.2240	–	–	–
Rb_2Se	a_o	7.984	8.02[c]	–	–
	E_0	−16,783.4194	–	–	–
	B_o	14.1218	–	–	–
	B'	3.7542	–	–	–

[a] Ref. [30].
[b] Ref. [9].
[c] Ref. [31].
[d] Ref. [13].
[e] Ref. [12].
[f] Ref. [14].
[g] Ref. [15].

While calculating structural properties of M_2Se crystals in anti-CaF_2 structure type, volume optimization was performed using WC GGA exchange-correlation functional. Equilibrium lattice constants (a_o), total energies (E_0), bulk modulus (B_o) and its pressure derivatives (B') have been calculated by fitting Murnaghan equation of state [23] to the total energy versus volume curve. Table 1 show the results obtained in present work for lattice constants and bulk moduli of alkali metal selenides along with available theoretical and experimental data. It can be readily seen that our calculated lattice parameters are in excellent agreement with experimental values. Since no experimental data is available for B_o and its pressure derivative for these compounds and also because computationally obtained second derivatives are more susceptible to numerical inaccuracies, no comparison as to the performance of FP-LAPW results for these parameters can be made with other theoretical results in general and TB-LMTO results in particular. As observed in the case of alkali metal oxides and sulfides, the lattice parameters and total energies of selenides of alkali metal increase and the bulk modulus decreases in going from lithium to rubidium selenide. It can be deduced from the decreasing values of bulk modulus of these materials that the compressibility of these materials increases with increasing cation radii.

3. Electronic properties

Full relativistic band structures calculations for alkali metal selenides were performed using WC GGA and EV GGA. However, only the band structure diagrams obtained using EV GGA are presented in Fig. 1. A close look at Fig. 2 clearly shows that lithium, potassium and rubidium selenides have an indirect fundamental energy band gap (X–Γ) whereas the selenide of sodium has a direct fundamental energy band gap (Γ–Γ). The valence band maximum

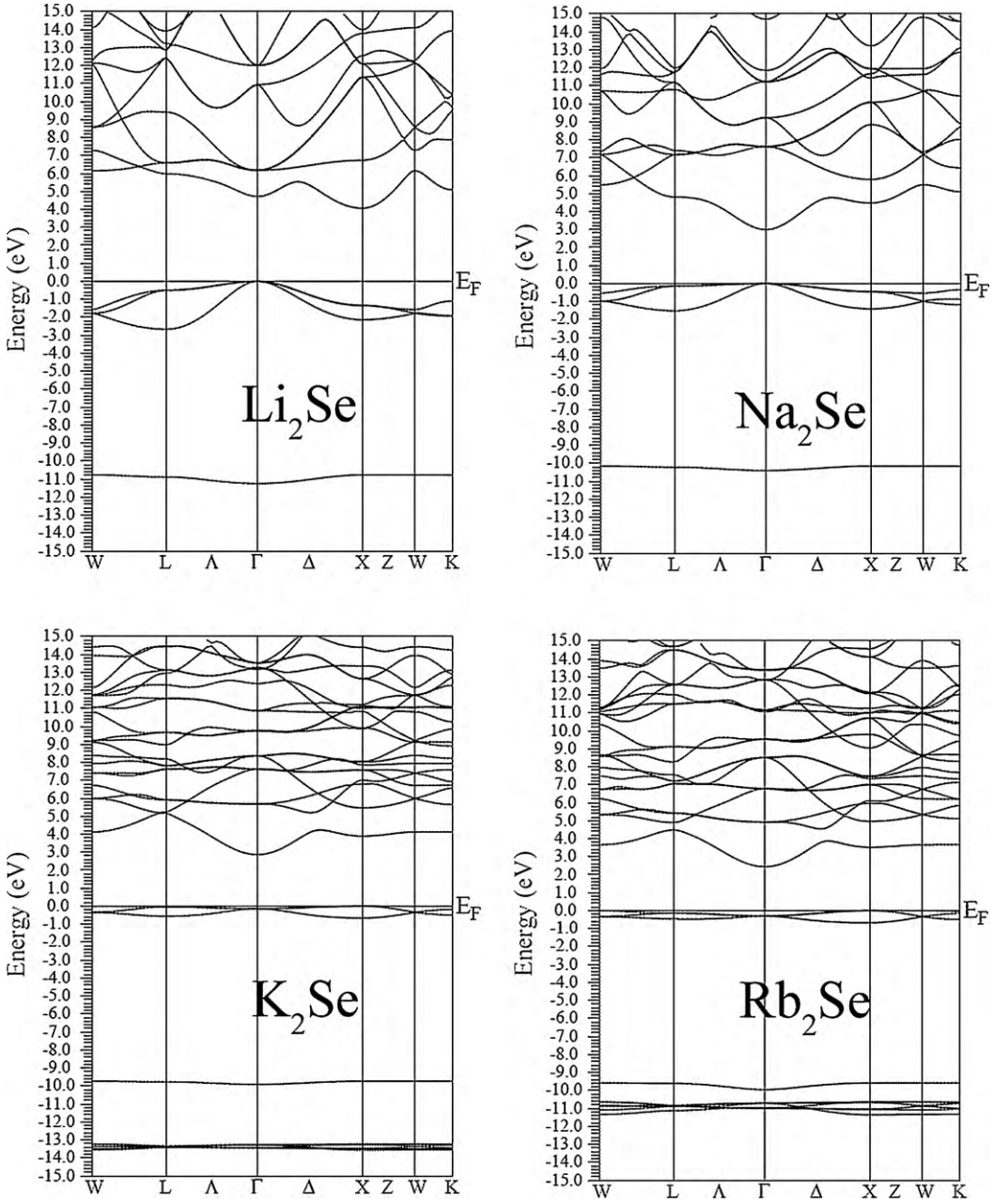

Fig. 2. Electronic band structure diagrams of Li_2Se, Na_2Se, K_2Se and Rb_2Se compounds obtained with EV GGA.

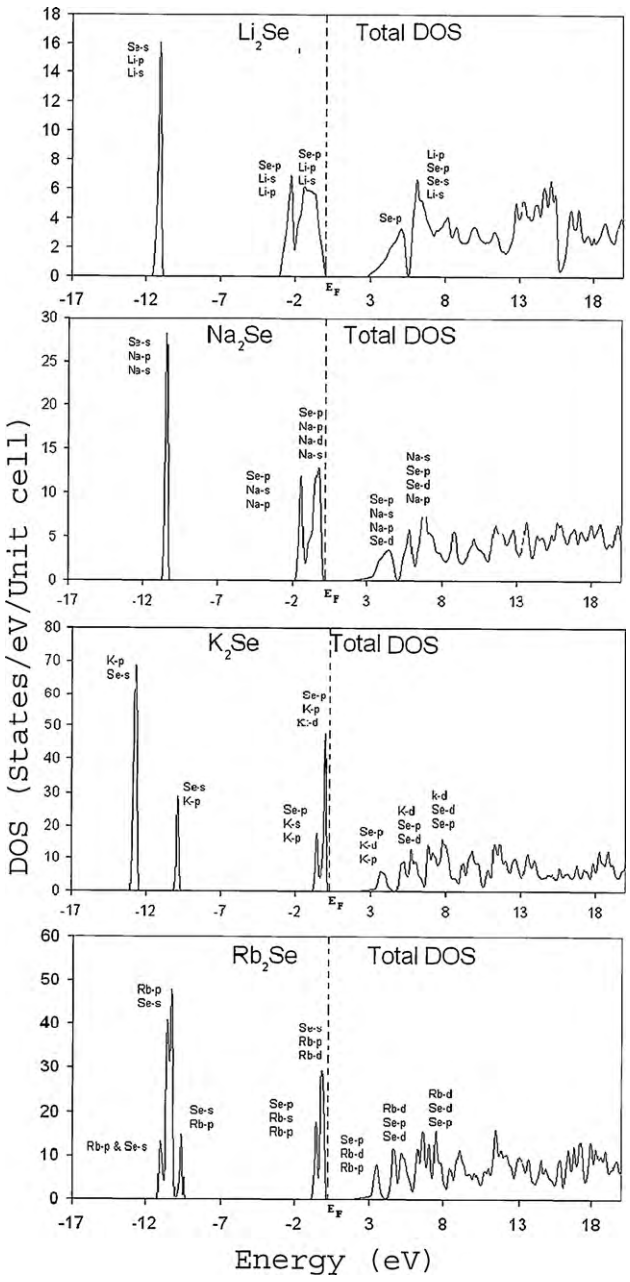

Fig. 3. Total DOS for alkali metal selenide crystals in anti-CaF_2 structure type. Contribution from various cation and anion states to the total density of states is presented over each peak.

for Li_2Se and Na_2Se compounds are located at the Γ-point and for K_2Se and Rb_2Se compounds it is located at the X-point. The conduction band minimum occurs at X-point for Li_2Se and at Γ-point for the selenides of Na, K and Rb. The Γ-point band degeneracy is also evident for all materials under study. In order to elucidate the contribution of various anion and cation states to the electronic structure of these materials and the nature of fundamental energy band gaps outlined above more clearly, total density of states (DOS) with contribution from individual cation and anion states of these materials has been presented in Fig. 3.

The lowest energy band for Li_2Se and Na_2Se are located at −11.22 eV and −10.43 eV, respectively which are mainly due to the anion s states. In case of K_2Se the lowest energy band at −9.82 eV is due to anions s states and the energy band at −13.25 eV is due to cation p states. For Rb_2Se the lowest energy band appearing at −9.74 eV is due to anion s states whereas the energy band at −10.22 eV is due to cation p states. It is evident that for the selenides of lithium and sodium the main contribution to the lowest energy band comes from the anions, whereas for K_2Se and Rb_2Se the lowest energy band splits into individual contributions from cation and anion. Unlike the oxides of alkali metal, the Se s states contribution to lowest energy band lie above the K and Rb p states contribution on the energy scale. Most of the contribution to the valence band width (VBW) comes from the anion p states in all these materials with minor contributions from s and p like states of Li, Na, K and Rb. Furthermore, the cation s like states contribute more to the lower energy band of VBW and cation p states contribute more to the upper energy band of VBW. The conduction band is a complex mixture of p and d states of anions and s, p and d states of cation. It is evident that with increasing size of cation the band structure becomes more and more complex and the lowest energy band starts to split. This may be due to the hybridization caused by increasing anion radius.

Table 2
Electronic band gap values calculated in present work using WC and EV GGA for alkali metal selenides along with TB-LMTO results.

Crystals		Energy band gap, E_g (eV)		Valence band width, E_v (eV)
		Γ–Γ	X–Γ	
Li_2Se	Present work:			
	WC GGA	3.18	2.82	2.42
	EV GGA	4.73	4.08	2.16
	TB-LMTO[a]	3.457	2.748	1.725
Na_2Se	Present work:			
	WC GGA	1.99	2.51	1.61
	EV GGA	2.98	3.15	1.36
	TB-LMTO[a]	2.598	3.133	0.610
K_2Se	Present work:			
	WC GGA	2.24	1.94	0.74
	EV GGA	2.97	2.84	0.67
	TB-LMTO[a]	2.272	2.190	0.106
Rb_2Se	Present work:			
	WC GGA	2.17	1.84	0.78
	EV GGA	2.73	2.42	0.66
	TB-LMTO[a]	–	–	–

[a] Ref. [15].

In Table 2 we summarize the calculated values for the energy band gaps (Γ–Γ and X–Γ) and VBW of M_2Se compounds. As expected, the values for energy gaps of all alkali metal selenides obtained with WC exchange-correlation energy functional are lower in value than that obtained by using EV functional. One can observe that the fundamental energy band gap for these compounds decreases as one goes from Li to Rb. Increasing atomic number of cations may be the cause for this, because the conduction band minimum tends to push its way downwards to the valence band as number of electrons in cation increase. The fundamental energy band gap values of all the materials obtained using WC GGA less than the corresponding TB-LMTO results whereas those of EV GGA are higher. On the other hand, values of VBW calculated using FP-LAPW method have a higher magnitude as compared to the TB-LMTO results.

In order to validate the applicability of the calculation method used in this study, a comparison of calculated electronic band structure parameters with experimental data is strongly needed. However, since no experimental data is available for the electronic band structure parameters of these materials, the validation of our calculations can only be made if the trends observed in band structure parameters of alkali metal selenides obtained using FP-LAPW method in this study are consistent with that observed for other dialkali monochalcogenides using first-principles techniques.

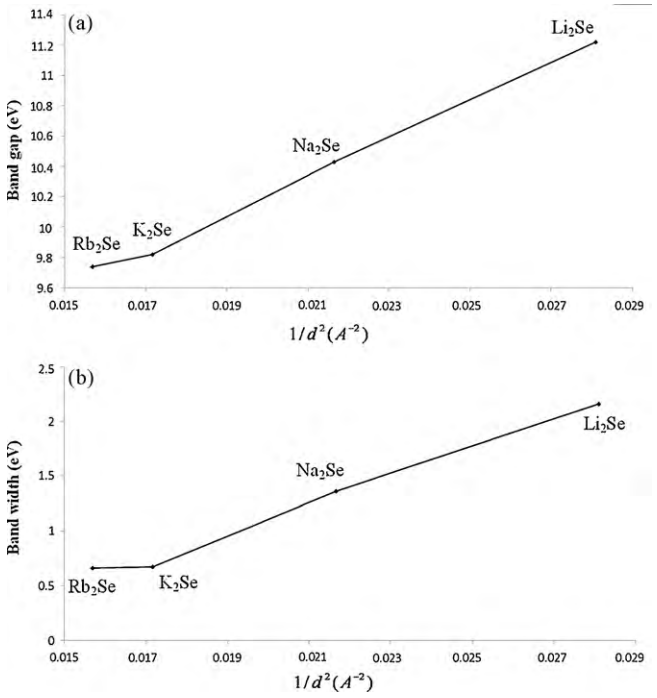

Fig. 4. (a) Calculated Se *s*–Se *p* band gap showing a linear dependence on $1/d^2$. (b) Calculated Se *p* valence band width (VBW) showing a linear dependence on $1/d^2$. *d* is the nearest-neighbor selenium distance.

Furthermore, we should also analyze the trends observed in available experimental studies of the electronic properties of dialkali monochalcogenides to support the performance of the calculation method used herein. From theoretical point of view, the studies performed by Khachai et al. [22] for alkali metal sulfides have shown that the VBW, the Γ–Γ and X–Γ band gaps decrease with increasing size of cation. A similar behavior can be observed (see Table 2) in both FP-LAPW results obtained for the above-mentioned band structure parameters of alkali metal selenides.

From experimental point of view, it has been established for alkali metal oxides [24] that the intervalence band gap at Γ-point of ionic compounds depends upon the overlap interactions between adjacent anions and not on the nearest-neighbor metal cations. Since the interatomic interactions are proportional to the reciprocal of anion–anion distance squared ($1/d^2$) [25], the band gap between the anion *s* and anion *p* states should also show linearly dependence on this quantity. Fig. 4(a) shows that there is a very strong linear dependence of the Se *s*–Se *p* band gap on $1/d^2$. Similar trend can be seen in the Se *p* VBW (Fig. 4(b)), which, like the band gap is linearly dependent upon the nearest-neighbor Se atom interactions. In addition to these dependencies we can also observe that the increase in band gap and VBW values between Rb_2Se and K_2Se is less as compared to that observed between K_2Se and Li_2Se. This is because the band structure of K_2Se and Rb_2Se has similar profile as compared to other two members of this family due to the large size of their cations.

4. Optical properties

4.1. Dielectric function and absorption coefficient

In solid-state materials various interband and intraband optical transitions are possible. To completely identify these transitions, one needs to compute tensor components of the dielectric function $\varepsilon(\omega)$. The intraband transitions are only important in case of metals whereas the interband transitions can be further divided into direct and indirect transitions. It is usual to neglect the indirect interband transitions since they are only involved in scattering of phonons and do not contribute to $\varepsilon(\omega)$. Since alkali metal selenides have cubic symmetry and can be treated as isotropic in relation to propagation of light, we need to compute only one component of the dielectric tensor. The imaginary part ($\varepsilon_2(\omega)$) of the incident photon's frequency (ω) dependent complex dielectric function is given by [26]:

$$\varepsilon_2(\omega) = \frac{e^2\hbar}{\pi m^2\omega^2}\sum_{v,c}\int_{BZ}[|M_{cv}(k)|^2]\delta[\omega_{cv}(k)-\omega]\ d^3k \quad (1)$$

The integral is over the first Brillouin zone. $M_{cv}(k) = \langle u_{ck}|\delta\cdot\nabla|u_{vk}\rangle$, where δ is the potential vector defining electric field, are the momentum dipole elements that are matrix elements for direct transitions between valence $|u_{vk}\rangle$ and conduction $\langle u_{ck}|$ band states, and the energy $\hbar\omega_{cv} = E_{ck} - E_{vk}$ is the corresponding transition energy. The real part of the dielectric function can be obtained from the imaginary part using the Kramers-Kronig relation [27],

$$\varepsilon_1(\omega) = 1 + \frac{2}{\pi}P\int_0^\infty \frac{\omega'\varepsilon_2(\omega')}{\omega'^2-\omega^2}\ d\omega' \quad (2)$$

where *P* is principle value of the integral. In order to accurately calculate $\varepsilon_1(\omega)$, we have calculated $\varepsilon_2(\omega)$ up to 65 eV and have used this value as truncation energy in Kramers-Kronig relation to ensure convergence in the Kramers-Kronig transformation. Fig. 5 displays calculated real and imaginary parts of dielectric function for M_2Se compounds for the incident photon's energy up to 35 eV. For these calculations a dense mesh of uniformly distributed **k**-points was used. As EV GGA seems to give better results for band structure calculations compared to WC functional, only the EV GGA has been used to perform optical properties calculations.

Since the imaginary part of dielectric function is directly related to the optical absorption in materials, a quick look at Fig. 5 reveals that lithium and sodium selenides should absorb strongly in the region between 2 eV and 15 eV. Almost same primary absorption regions are expected for the selenides of potassium and rubidium along with secondary absorption regions located between 15 eV and 27 eV. The critical points structures in $\varepsilon_2(\omega)$ for Li_2Se, Na_2Se, K_2Se and Rb_2Se occur at 4.84 eV, 3.15 eV, 2.81 eV and 2.59 eV, respectively. The increase in the curves beyond critical point values is due to the increasing number of points contributing to $\varepsilon_2(\omega)$. First peak appearing at 6.59 eV for Li_2Se is for the Γ_v–Γ_c splitting which gives rise to direct optical transitions between the highest valence band and lowest conduction band. The small bents around 7.8 eV are related to direct optical transition along the Λ and Δ directions. In case of Na_2Se the first peak appearing at 5.13 eV corresponds to direct transitions about the *L*-direction. The second peak, which is the main peak, located at 6.71 eV is due to direct Γ–Γ transitions, whereas, the structure appearing at 7.55 eV corresponds to *X*–*X* transitions. The remaining two selenides of alkali metal have common features in their spectrum and the peaks for K_2Se/Rb_2Se located at 4.55 eV/4.09 eV, 5.64 eV/5.21 eV (the main peaks) and 8.27 eV/7.71 eV originate from direct transitions along *W*–*W*, Γ–Γ and upper valence band and the conduction band along the Λ and Δ directions. The peaks appearing beyond 15 eV are related to the transitions between low laying valence band and conduction band along Λ, Δ and *W*–*L* directions.

From the results for the real part of the dielectric function, it can be seen that in case of Li_2Se and Na_2 Se peaks appear at around 5 eV followed by a steep decrease eventually making $\varepsilon_1(\omega)$ negative, it reaches a minimum and then slowly increases toward zero followed by a very slow increase for higher energies. In case of K_2Se and Rb_2 Se peaks appear again at around 4 eV but do not decrease as steeply as observed in the case of Li and Na selenides, however, $\varepsilon_1(\omega)$ does become negative around 8 eV and reaches a

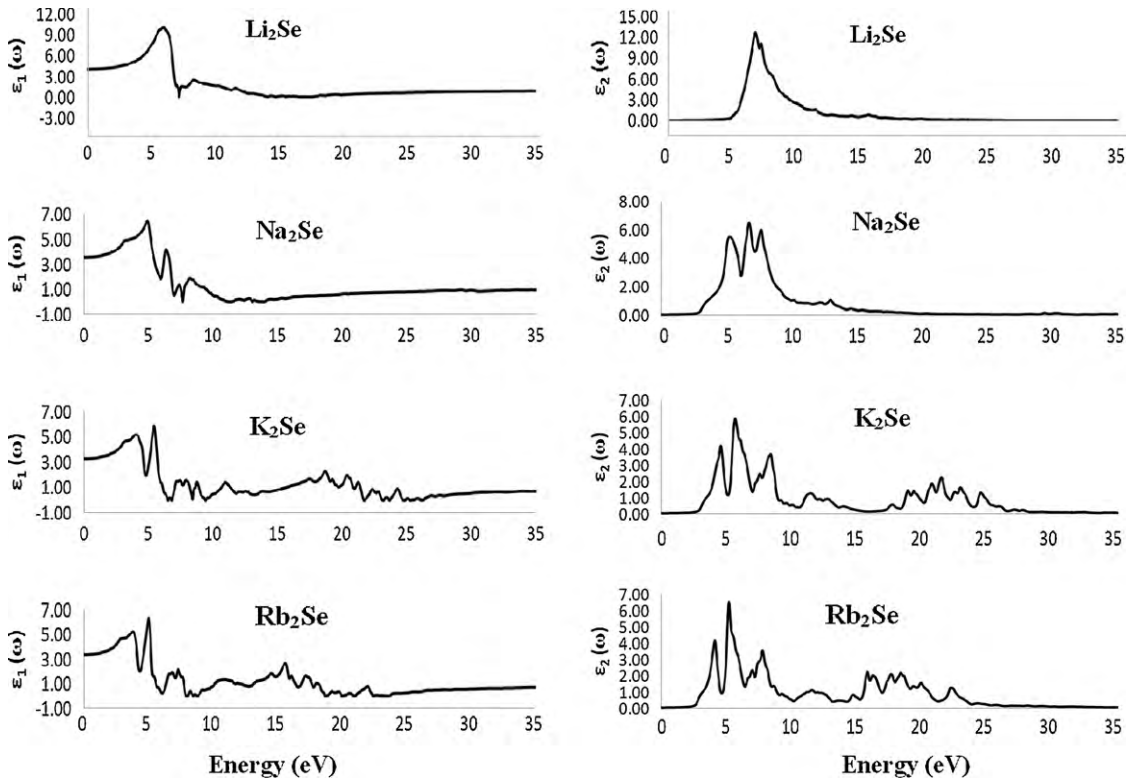

Fig. 5. Calculated real ($\varepsilon_1(\omega)$) and imaginary ($\varepsilon_2(\omega)$) parts of the complex dielectric functions for radiations up to 35 eV for alkali metal selenides.

minimum and then slowly increases toward zero and passes it and then another minimum appears at around 23 eV for these materials and then again a slow increase and a pass over from zero level at higher energies. From the knowledge of $\varepsilon_1(\omega)$ we can determine two important quantities namely the static dielectric constant $\varepsilon_1(0)$ which is defined as the low energy limit of real part of dielectric function and the screened plasma frequencies that are given by the zero crossing of $\varepsilon_1(\omega)$ at high frequencies. As phonon contribution to the dielectric screening is not included, the static dielectric constant corresponds to static optical dielectric constant ε_∞. The calculated dielectric constants for Li_2Se, Na_2Se, K_2Se, and Rb_2Se are 3.97, 3.51, 3.25 and 3.35, respectively and the screened plasma frequencies are 2.54×10^{16} rad/s, 2.04×10^{16} rad/s, 3.95×10^{16} rad/s and 3.55×10^{16} rad/s, respectively.

In Fig. 6 we present the absorption coefficients, $I(\omega)$, of M_2Se semiconductors. A comparison with Fig. 5 justifies the above-mentioned strong absorption regions for these materials. These absorption regions are the incident photon energy ranges in which these materials should be optically excited. Our results show that lithium selenide has a sharp edge of absorption coefficient below 5 eV which goes backwards to around 2.5 eV as we go from Na → K → Rb. This sharp edge of absorption coefficient should be expected for semiconductor materials since electromagnetic radiations which do not have sufficient energy to raise an electron across the band gap, does not get absorbed in that material. Strong absorption regions for M_2Se compounds occur at around 8 eV suggest that these materials may find applications in ultraviolet optoelectronic devices. In addition to the above-mentioned absorption region, the potassium and rubidium selenides have large values of absorption coefficient also at higher energy ranges. The absorption peaks around 20 eV show that K_2Se and Rb_2Se compounds may also find applications in ultraviolet space technology devices that require absorption of extreme-ultraviolet radiations. A comparative analysis of absorption spectra with electronic band structure (Fig. 2) reveals the manner in which incident radiation may get absorbed in these materials. It is obvious that Se *p* states and metal atom *p* and *d* states play a major role in these optical transitions as initial and final states for Na_2Se, K_2Se and Rb_2Se. In case of Li_2Se where Li does not have any *d* states laying near in energy to the Fermi level, this contribution is reasonably small. In this study, spin-orbit coupling calculations for these materials have not been performed, since it has been previously shown [22,28] that spin-orbit coupling changes the eigenvalues only by 0.1 eV, which is not significant for optical calculations.

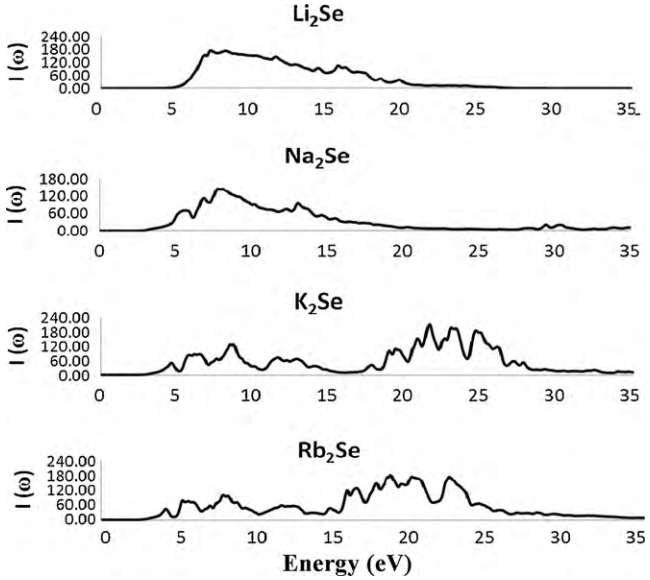

Fig. 6. The absorption coefficient (I) as a function of incident photon energy ($\hbar\omega$) for Li, Na, K and Rb selenides.

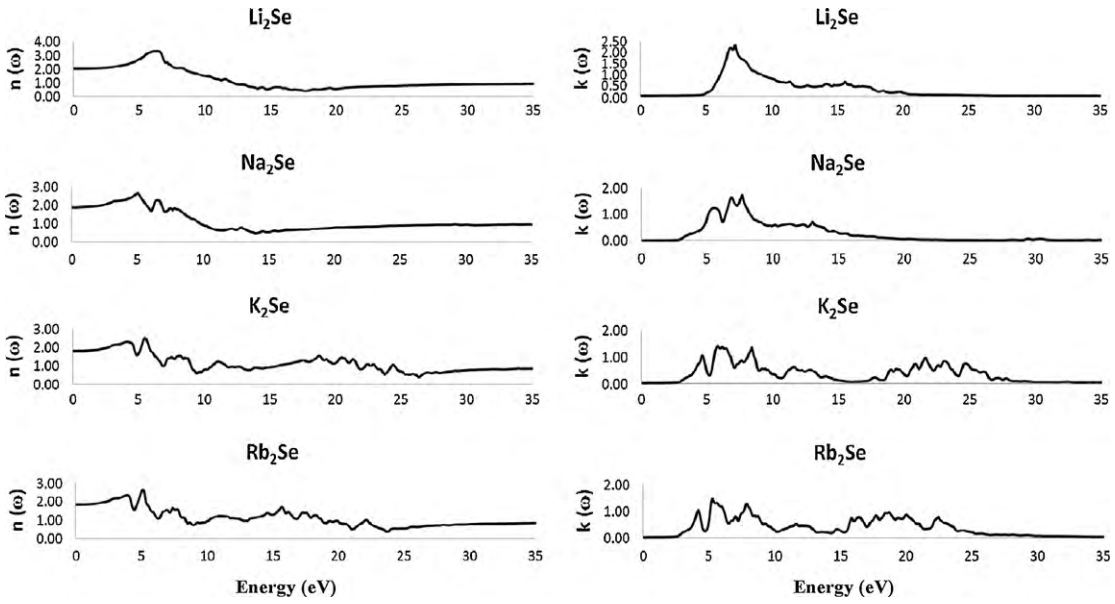

Fig. 7. The refractive index (n) and extinction coefficient (k) as a function of incident photon energy ($\hbar\omega$) for alkali metal selenides.

4.2. Refractive index, extinction coefficient and reflectivity

Knowing the complex dielectric tensor one can calculate various optical constants such as refractive index (n) and extinction coefficient (k). The knowledge of the former is essential for optical properties of materials and the latter directly describes the attenuation of electromagnetic waves inside a materials. The relationship between these quantities and the real and imaginary parts of dielectric function are written as: $\varepsilon_1(\omega) = n^2 + k^2$ and $\varepsilon_2(\omega) = 2nk$. Fig. 7 displays the variation of refractive index and extinction coefficient for alkali metal selenides obtained by the FP-LAPW calculation as a function of incident photon energy. Our calculations show that refractive index closely follows $\varepsilon_1(\omega)$, whereas, extinction coefficient changes as $\varepsilon_2(\omega)$. An analysis of the variation of extinction coefficients with energy reveals that the attenuation of alkali metal selenides decreases from Li_2Se to Rb_2Se.

The calculated reflectivity spectra for the compounds under investigation are given in Fig. 8, which shows that the spectra for Li and Na selenides resemble and those of K and Rb selenide are similar. The reflectivity for all these materials starts at 10%. Our

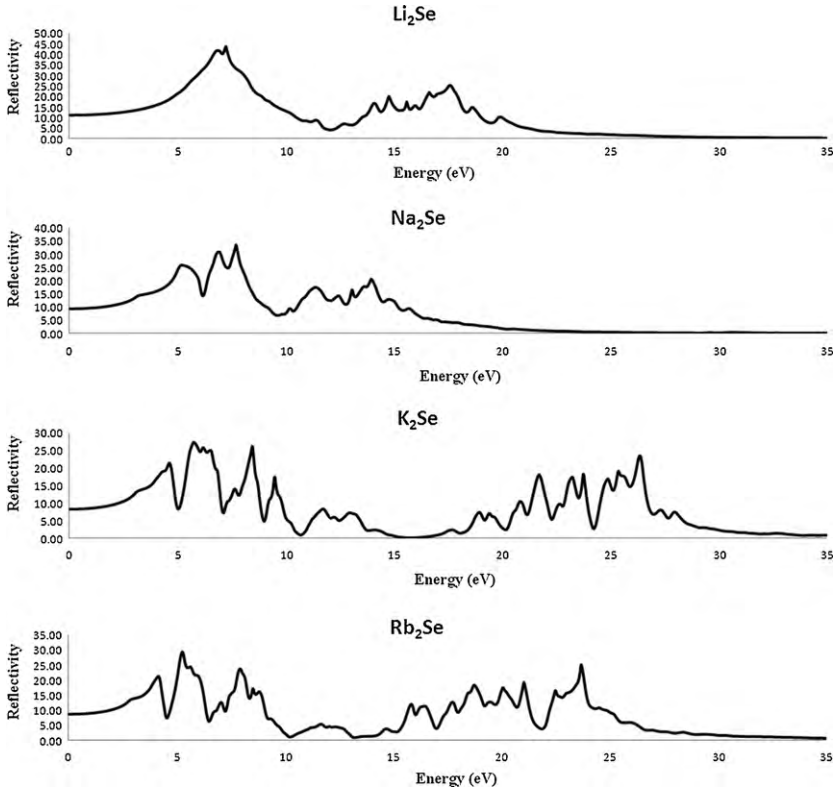

Fig. 8. The reflectivity of alkali metal selenide crystals as a function of incident photon's energy.

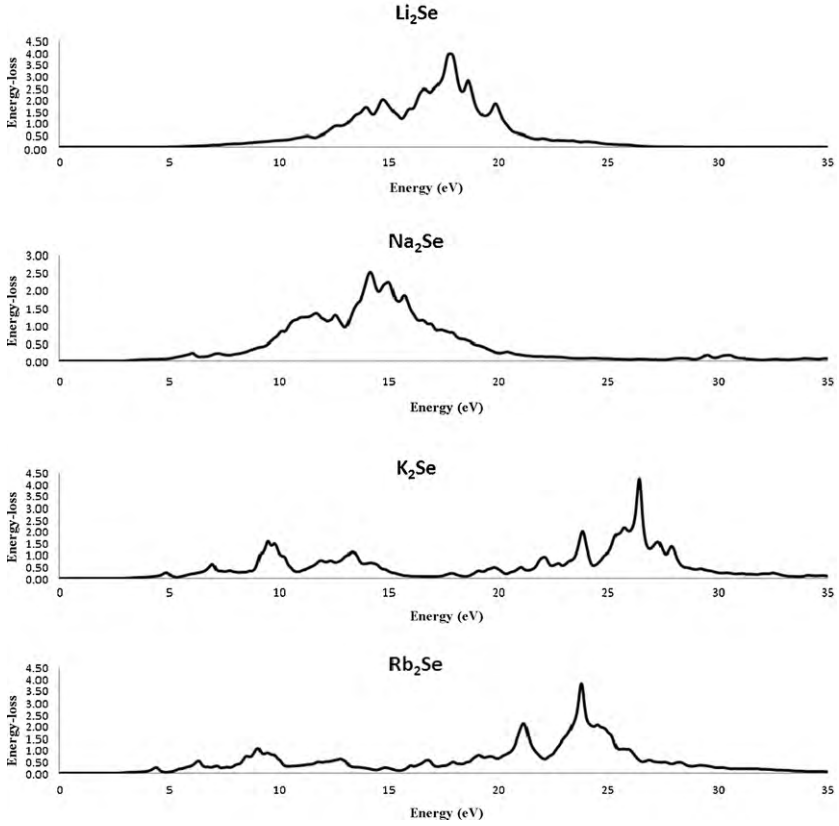

Fig. 9. Electron energy-loss function calculated using FP-LAPW method for Li, Na, K and Rb selenides.

calculated reflectivity for Li_2Se, Na_2Se, K_2Se and Rb_2Se reach maximum values of around 50%, 35%, 30% and 25% at 6.89 eV, 7.63 eV, 5.61 eV and 5.16 eV, respectively. For Li_2Se and Na_2Se there is a constant dip up to 11.79 eV and 9.32 eV, respectively followed by smaller peaks up to 20 eV for these materials after that the reflectivity becomes zero. In case of the remaining two alkali metal selenides the reflectivity almost falls off to zero at three points and shows irregular behavior throughout the energy range.

4.3. Electron energy-loss function

The electron energy-loss function describes the interaction by which energy is lost by a fast moving electron travelling the material. The interactions may include phonon excitation, interband and intraband transitions, plasmon excitations, inner shell ionizations and Čerenkov radiations. The energy loss is usually large at the plasma frequencies [29]. The energy-loss spectra shown in Fig. 9 for the compounds under study show the peaks at different energy ranges corresponding to electronic excitations of different orbitals. Energy-loss spectra do not show maxima for zeros of $\varepsilon_1(\omega)$ because $\varepsilon_2(\omega)$ is large at these energies. Broad band between 7 eV and 21 eV appear for Li_2Se and Na_2Se whereas for K_2Se and Rb_2Se these appear between 18 eV and 28 eV. The peaks of our calculated energy-loss function (Fig. 9) have maxima at 17.62 eV, 14.00 eV, 26.38 eV and 23.68 eV for selenides of Li, Na, K and Rb, respectively, which fits very well with the rapid decrease in reflectivity in Fig. 8 and corresponds with transitions from occupied Se and metal atom *s* states to the anion *p* like states laying below the valence band to an empty conduction band. These peaks have intensities several orders of magnitude higher than the other peaks which are caused by collective oscillation of the loosely bound electrons that runs as a longitudinal wave through the volume of the crystal with a characteristic plasma frequency outlined earlier.

5. Conclusions

In this study we have applied FP-LAPW method to investigation electronic and optical properties of alkali metal selenides (M2Se) [M: Li, Na, K, Rb] using WC and EV generalized gradient approximation exchange-correlation functionals in the framework of DFT. In the light of earlier studies of alkali metal oxides and sulfides it seems that EV GGA tends to give better results for electronic band structure parameters of these materials which are larger as compared to values obtained with TB-LMTO method. From the electronic band structure of these compounds it has been established that fundamental energy band gap for the common anions of all alkali metals decrease as we go from Li_2Se to Rb_2Se. We have analyzed various interband transitions of these materials in the light of electronic band structure and DOS of these materials which show that these materials are suitable candidates for ultraviolet optoelectronic devices. The structure of complex dielectric function has been analyzed to identify the possible optical transitions in these materials. The Se *p* states and metal atom *p* and *d* states play a major role in these optical transitions as initial and final states. The static optical dielectric constant and plasma frequencies of these materials have been predicted. In addition to above-mentioned optical parameters, we have also computed refractive index, attenuation, reflectivity and electron energy-loss function for alkali metal selenides. It is hoped that the data presented in this work will serve as reference data for future experimental and theoretical studies of these materials.

References

[1] T. Minami, A. Hayashi, M. Tatsumisago, Solid State Ionics 136 (2000) 1015.
[2] J.S. Esher, Semiconductors and Semimitals, Academic Press, New York, 1981, p. 195.
[3] C. Gosh, Phys. Thin Films-Photoemissive Mater. 12 (1982) 75.

[4] D. Bisero, B.M. van Oerle, G.J. Ernst, J.W.J. Verschuur, W.J. Witteman, Appl. Phys. Lett. 69 (1996) 3641.
[5] D. Bisero, B.M. van Oerle, G.J. Ernst, J.W.J. Verschuur, W.J. Witteman, J. Appl. Phys. 82 (1997) 1384.
[6] C.T. Campbell, J. Catal. 94 (1985) 436.
[7] P. Soukiassian, H.I. Starnberg, in: H.P. Bonzel, A.M. Bradshaw, G. Ertl (Eds.), Physics and Chemistry of Alkali Metal Adsorption, Elsevier, Amsterdam, 1989, p. 449.
[8] S. Hull, T.W.D. Farley, W. Hayes, M.T. Hutchings, J. Nucl. Mater. 160 (1988) 125.
[9] E. Zintle, A. Harder, B. Dauth, Z. Elektrochem. 40 (1934) 588.
[10] J. Sangster, A.D. Pelton, J. Phase Equilib. 18 (1997) 190.
[11] A.K. Koh, Phys. Stat. Sol. (b) 210 (1999) 31.
[12] V.K. Jain, J. Shanker, Phys. Stat. Sol. (b) 114 (1982) 287.
[13] S.D. Chaturvedi, S.B. Sharma, P. Paliwal, M. Kumar, Phys. Stat. Sol. (b) 156 (1989) 171.
[14] A. Melillou, B.R.K. Gupta, Czech. J. Phys. 41 (1991) 813.
[15] R.D. Eighitaj, G. Jaiganesh, G. Kalpana, Int. J. Mod. Phys. B 23 (2009) 5027.
[16] P. Blaha, K. Schwarz, G.H. Madsen, D. Kvasnicka, J. Luitz, FP-L/APW+lo Programe for Calculating Crystal Properties (K. Schwarz, Techn WIEN2K, Austria), 2001.
[17] P.A.M. Dirac, Proc. Camb. Philos. Soc. 26 (1930) 376.
[18] Z. Wu, R.E. Cohen, Phys. Rev. B 73 (2006) 235116.
[19] J.P. Perdew, K. Burke, M. Ernzerhof, Phys. Rev. Lett. 77 (1996) 3865.
[20] E. Engel, S.H. Vosko, Phys. Rev. B 47 (1993) 13164.
[21] M. Moakafi, R. Khenata, A. Bouhemadou, H. Khachai, B. Amrani, D. Rached, M. Rèrat, Eur. Phys. J. B: Condens. Matter Complex Syst. 64 (2008) 35.
[22] H. Khachai, R. Khenata, A. Bouhemadou, A. Haddou, A.H. Reshak, B. Amrani, D. Rached, B. Soudini, J. Phys.: Condens. Matter 21 (2009) 095404.
[23] F.D. Murnaghan, Prot. Natl. Acad. Sci. U.S.A. 30 (1944) 244.
[24] E.A. Mikajlo, H.E. Dorsett, M.J. Ford, J. Chem. Phys. 120 (2004) 10799.
[25] W.A. Harrison, Electronic, Structure and the Properties of Solids, Dover, New York, 1989.
[26] C. Ambrosch-Draxl, J.O. Sofo, Comp. Phys. Commun. 175 (2006) 1.
[27] F. Wooten, Optical Properties of Solids, Academic Press, New York, 1972.
[28] R. Ahuja, O. Eriksson, B. Johansson, S. Auluck, J.N. Wills, Phys. Rev. B 54 (1996) 10419.
[29] M. Xu, S.Y. Wang, G. Yin, J. Li, Y.X. Zheng, L.Y. Chen, Appl. Phys. Lett. 89 (2006) 151908.
[30] R. Anthony, Solid State Chemistry and its Applications, John Wiley and Sons, 1991, ISBN 0471908746.
[31] S.P. Yatsenko, A.N. Kunzetsov, K.A. Chontonov, Inorg. Matter 13 (1977) 4.